Electronic Supplementary Information for

Insight into delivery channel and selectivity of multiple binding sites in bovine serum albumin towards naphthalimide-polyamine derivatives

Fangfang Fan,[a] Yuan Zhao *[b] and Zexing Cao *[a]

[a]State Key Laboratory of Physical Chemistry of Solid Surfaces and College of Chemistry and Chemical Engineering, Xiamen University, Xiamen 361005, China

[b]The Key Laboratory of Natural Medicine and Immuno-Engineering, Henan University, Kaifeng 475004, China

*E-mail: zhaoyuan@henu.edu.cn (Y. Zhao) *E-mail: zxcao@xmu.edu.cn (Z. Cao)

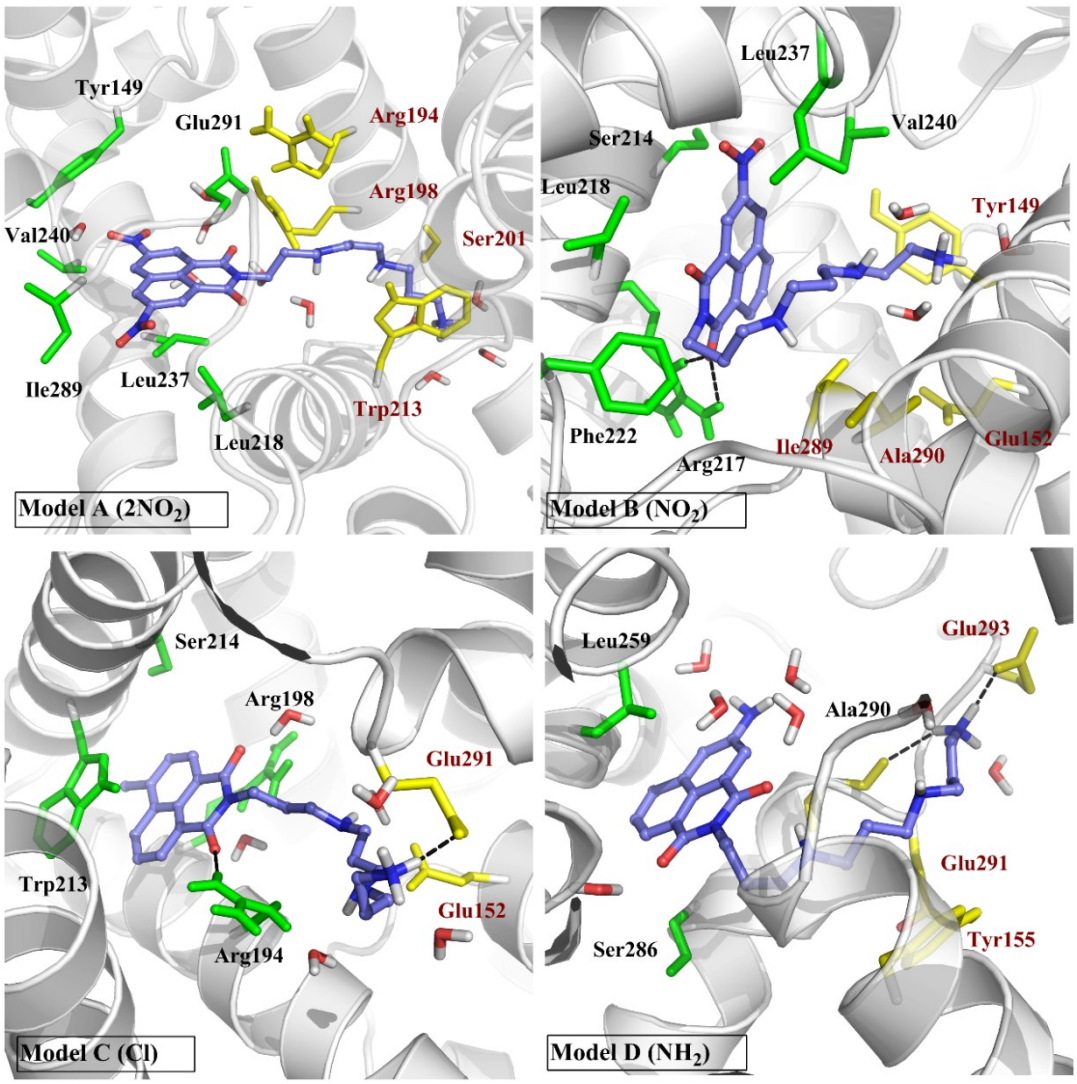

Fig. S1 The structures of different complex after molecular dynamics in DSI. The residues close to the head part of the complex are colored in green, and the ones close to the tail are yellow. Model A with two strong electron-withdrawing groups (NO_2), Tyr149, Leu218, Leu237, Val240, Ile289 and Glu291 form a cavity to localize the head of the ligand. In addition to this, the strong cation-π interaction is found between the aromatic ring of Trp213 and the tail of the ligand. Arg194, Arg198, Ser201 and Trp213 that have influence to the tail fixation further strengthen the combining capacity. The same as Model A-$2NO_2$, there also have some main residues around the head of the Model B-NO_2, including a hydrogen bond between the Arg217 and the head part of the ligand, although the overall contribution of these main residues reduces compare with the Model A-$2NO_2$. This is consistent with the result above that the larger number of the electron-withdrawn groups in the conjugates have better

combing pattern. Model C with a weak electron-withdrawn group (Cl) further decreases the number of main residues around the head part. Model D with electron-donor groups (NH_2) distinctly cuts off the number of main residues resulting to weak the binging capacity.

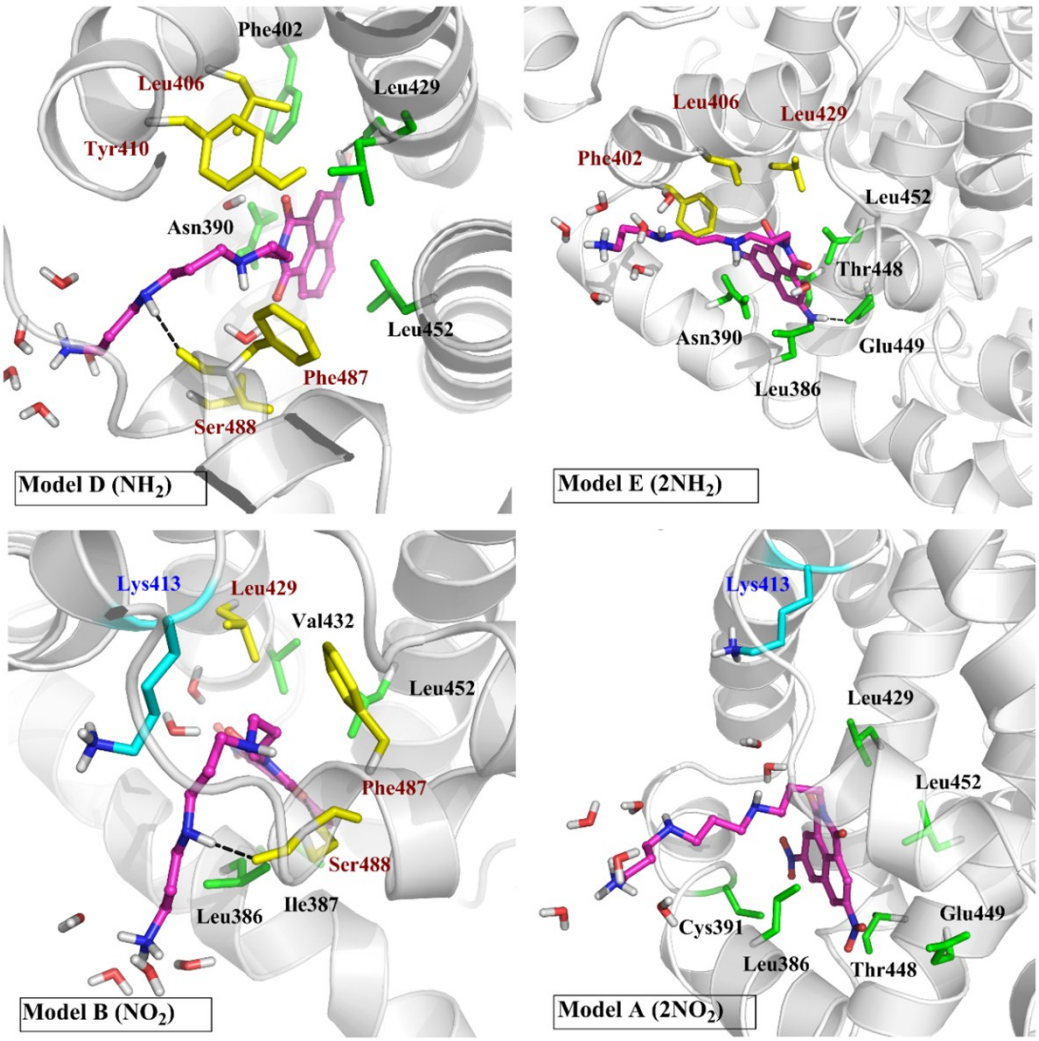

Fig. S2 The structures of different complex after molecular dynamics in DSII. The residues close to the head part of the complex are colored in green, and the ones close to the tail are yellow. Model D-NH_2, substrate deeps into the drug site firmly with the main residues located at the head and tail that makes a great contribution to bind, including a distinct hydrogen bond between the amino group of the ligand and Leu429. As to Model E-$2NH_2$, steric effect affects the ability to combine due to the space limitation of the pocket to a large extent. Although a distinct hydrogen bond is found between the one of the amino group of the substrate and Glu449, there are another four residues (Leu386, Asn390, Thr448 and Leu452) are likely to stabilize the head of ligand. Model B-NO_2 and Model A-$2NO_2$, both have electron-withdrawn groups, can't perfect amalgamation with the DSII, since Lys413 located at the door of the pocket plays a repulsive role with the long polyamine tail that weaken the binging interaction.

Table S1. Data collection of BSA protein from protein data bank.

BSA				
PDB code	3V03	4F5S	4JK4	4OR0
Deposited	2011/12	2012/5	2013/3	2014/2
Resolution (Å)	2.7	2.5	2.7	2.6
Author (group)	Minor, W.	Bujacz, A.	Bujacz, A.	Sekula, B.
HSA				
PDB code	1E78	1H9Z	2BXD	2VDB
Deposited	2000/8	2001/3	2005/7	2007/10
Resolution (Å)	2.6	2.5	3.1	2.5
Author (group)	Curry, S.	Curry, S.	Curry, S.	Nordberg, P.

Table S2. Statics of 45 trajectories for the substrate delivery using RAMD/MD.

Drug site I			**Drug site II**		
Pathways	**Number of trajectories**	**Possibility**	**Pathways**	**Number of trajectories**	**Possibility**
Pa_1	29	64.4%	**Pa_2**	45	100%
Pb_1	11	24.4%			
Pc_1	5	11.1%			

Table S3. Energy analysis of complexes in DSI by MM/GBSA (kcal/mol).

Model	ΔG_{bind}	ΔE_{vdw}	ΔE_{ele}	ΔG_{GB}	ΔG_{SA}	ΔG_{gas}	ΔG_{sol}
Model A -2NO_2	-47.9	-67.7	-19.4	48.9	-9.7	-87.1	39.2
Model B -NO_2	-35.1	-49.4	-72.6	93.3	-6.4	-121.9	86.9
Model C -Cl	-36.6	-41.4	-61.6	71.6	-5.2	-103.0	66.4
Model D -NH_2	-25.9	-44.1	-37.8	63.2	-7.1	-82.0	56.1
Model E -2NH_2	-25.7	-44.1	-18.7	45.5	-8.4	-62.8	37.1

Table S4. Energy analysis of complexes in DSII by MM/GBSA (kcal/mol).

Model	ΔG_{bind}	ΔE_{vdw}	ΔE_{ele}	ΔG_{GB}	ΔG_{SA}	ΔG_{gas}	ΔG_{sol}
Model D -NH_2	-45.7	-49.4	-0.4	11.7	-7.6	-49.8	4.1
Model E -2NH_2	-36.9	-50.6	-3.4	25.9	-8.9	-54.0	17.1
Model C -Cl	-36.1	-43.3	-33.5	46.1	-5.4	-76.8	40.7
Model B -NO_2	-34.9	-49.2	-0.2	21.9	-7.4	-49.4	14.5
Model A -2NO_2	-33.8	-57.0	-6.6	38.0	-8.3	-63.5	29.7

Table S5. Energy analysis of Model F in two drug sites by MM/GBSA (kcal/mol).

Model	$\Delta G_{binding}$	ΔE_{vdw}	ΔE_{ele}	ΔG_{GB}	ΔG_{SA}	ΔG_{gas}	ΔG_{sol}
Model F-DSI	-49.8	-60.8	-15.9	37.0	-10.2	-76.7	26.8
Model F-DSII	-42.0	-55.0	-10.9	33.1	-9.2	-65.9	23.9